Ind. J. Pharm. Edu. Res., 2026; 60(4s):s1486-s1497.
https://www.ijper.org

Original Article

Optimization of Palbociclib Nano Structured Lipid Carriers Loaded Transdermal Patch with Comprehensive *ex vivo* Skin Permeation and Retention Research for Management of Breast Cancer

Anilkumar Shinde[1], Nikita Gurav[1,2,*], Harinath More[1]

[1]Department of Pharmaceutics, Bharati Vidyapeeth College of Pharmacy, Kolhapur, Maharashtra, INDIA.
[2]Department of Pharmaceutics, Dr. Shivajirao Kadam College of Pharmacy, K. Digraj, Sangli, Maharashtra, INDIA.

ABSTRACT

Background: Palbociclib (PCB), a selective cyclin-dependent kinase 4/6 prescribe for hormone receptor-positive breast cancer, has low oral bioavailability and dose-limiting systemic toxicity. **Objectives:** In order to achieve prolonged drug administration and improved transdermal penetration, the current work sought to create and optimize a transdermal patch containing PCB based on Nanostructured Lipid Carriers (NLCs). **Materials and Methods:** After being adsorbed onto Neusilin® US2, PCB-NLCs were embedded to transdermal patches made using the solvent-casting method. The concentrations of HPMC K100 and Eudragit RS100 were optimized using a 2^2 complete factorial design, with tensile strength and time needed for 90% drug release chosen as the crucial quality criteria. **Results:** The honed formulation showed high drug content uniformity, skin-compatible pH, consistent thickness, and outstanding mechanical flexibility. PCB found to release steadily over a 72-hr period *in vitro*, according to Higuchi diffusion kinetics. Additionally, compared to the free drug solution, *ex vivo* permeation tests utilizing goat skin showed a 2.4-fold increase in steady-state flow and a considerably shorter lag time. Skin retention studies, indicating significant drug deposition into epidermal and dermal layers confirmed development of an intradermal drug depot. MTT assay and stability report ensures retaining of antitumor action of PCB in NLC form embed in transdermal patch. **Conclusion:** All things considered, the developed NLC-based transdermal patch is a promising alternative delivery system for PCB, providing enhanced skin penetration, controlled and sustained drug release, and the potential to reduce systemic toxicity linked to traditional oral therapy in the treatment of breast cancer.

Keywords: Breast Cancer, Ex vivo Skin Permeation, Nano-structured Lipid Carriers, Palbociclib, Transdermal Patch.

Correspondence:
Ms. Nikita Gurav[1,2]
[1]Department of Pharmaceutics, Bharati Vidyapeeth College of Pharmacy, Kolhapur, Maharashtra, INDIA.
[2]Department of Pharmaceutics, Dr. Shivajirao Kadam College of Pharmacy, K. Digraj, Sangli, Maharashtra, INDIA.
Email: nikitagurav666@gmail.com

Received: 11-06-2026;
Revised: 06-07-2026;
Accepted: 29-08-2026.

INTRODUCTION

On February 3, 2015, the U.S. Food and Drug Administration approved Palbociclib (PCB) for the treatment of hormone receptor positive, HER2-negative breast sarcoma.[1,2] It functions as a targeted anticancer treatment because it selectively inhibits proteins known as CDK4/6, which are responsible for unchecked cancer cell division, particularly in hormone receptor-positive breast cancer, in contrast to conventional chemotherapy, which targets all rapidly dividing cells. By selectively inhibiting CDK4/6-mediated phosphorylation of retinoblastoma protein, thereby arresting cancer cells in the G1 phase it prevents tumor cell proliferation.[3] It is taken orally as a medication in the form of tablets or capsules. Within each 28-day treatment cycle, PCB is usually given as an OD dose for 21 days in a row, followed by a 7-day drug-free break.[4] After absorption it enters the bloodstream and acts throughout the body, including metastatic tumor sites.[5,6]

Despite its proven efficacy, dose-limiting hematological toxicities of PCB can impact multiple organs and systems throughout the body. The most common and notable systemic side effects include neutropenia, leukopenia, anemia and thrombocytopenia.[7-9] Moreover, oral PCB therapy is associated with significant pharmacokinetic limitations, including extensive first-pass metabolism mediated by CYP3A4, inter-patient variability in exposure, pH-dependent solubility and variable absorption in gastrointestinal conditions.[10-12] Since it belongs to BCS II its low water solubility results in rate limiting dissolution and absorption

DOI: 10.5530/ijper.20265560

after oral administration.[13] Oral absorption may vary due to food effects, gastric emptying time and intestinal conditions. Oral therapy of PCB may produce nausea, vomiting, diarrhea, stomatitis, frequent dosing requirement for long-term oral therapy may affect adherence in cancer patients. Additionally conventional oral dosage forms cannot effectively target tumor tissue specifically. Therefore, higher systemic exposure leads to lower site-specific delivery efficiency. This can even produce inconsistent plasma drug levels.

These drawbacks are major reason researchers investigate nano formulations and alternative drug delivery strategies capable of maintaining therapeutic plasma concentrations while minimizing systemic adverse effects.[14]

In recent research studies, scientists are investigating injectable nanoparticles,[13,15,16] liposomes,[17] Nanostructured Lipid Carriers (NLCs),[18-20] and other nano-carrier[21,22] systems to improve tumor targeting, bioavailability, and controlled delivery of PCB.

Because of their high drug loading capacity, improved stability, controlled release behavior, increased bioavailability, biocompatibility, and capacity to modify the therapeutic efficacy of low soluble anticancer drugs like PCB, NLCs are regarded as one of the best nano formulations. PCB-loaded NLCs demonstrated considerable promise for oral administration in the treatment of breast sarcoma in a recently published trial, improving medication delivery and reducing side effects.[19]

However, considering limitations of oral administration, we have explored non-invasive transdermal delivery of PCB that offers many advantages such as bypassing first-pass metabolism, reducing gastric discomfort, minimizing systemic toxicity, sustained and controlled drug input, improved patient compliance, and rapid termination of therapy if required.[23,24]

However, PCB's limited skin permeability and lack of water solubility make effective transdermal administration difficult. Through lipid-lipid interactions with the stratum corneum, NLCs have shown promise as carriers for improving the solubility and skin penetration of weakly water *in vitro* soluble medications.[25]

In our earlier published study, we have developed PCB-NLCs using Sterotex HM as solid lipid and Captex 300 as liquid lipid (9:1) and blend of Tween 80: Span 80 (4:1) and adsorbed onto Neusilin® US2.[18]

In order to determine its potential for long-term breast cancer treatment, the current study focuses on the formulation and optimization of a PCB-loaded NLC-based transdermal patch utilizing a full factorial design of experiments technique. This is followed by a thorough and *ex vivo* evaluation.

MATERIALS AND METHODS

PCBs were bought from Sigma Aldrich (Merck); Tween 80, HPMC K100, Span 80, Eudragit RS100, PVP K30, Oleic acid, Glycerol, and Formic acid were bought from LOBA Chemicals, Mumbai; Ethanol, Methanol (HPLC grade), Diethyl ether, and Hydrochloric acid were bought from S.D. Fine Chem, Mumbai.

Fresh goat ear skin used in this study for *ex vivo* skin permeation analysis was obtained from a local slaughterhouse as a by-product of routine commercial slaughter. Since no animals were sacrificed specifically for the study, Institutional Animal Ethics Committee approval was not required.

HPLC Analytical technique development

Using acetonitrile: water 70:30 containing 0.1% formic acid, the RP-HPLC method was developed and validated in compliance with ICH Q2(R1) guidelines, exhibiting accuracy, precision, linearity, specificity, robustness, and sensitivity for dependable PCB quantification.

Formulation of transdermal patches

Transdermal patches were made by solvent casting utilizing HPMC K100 and Eudragit RS100 as film-forming polymers, glycerol as a plasticizer, and oleic acid as a permeation enhancer after the compatibility of the chosen polymers with PCB was verified by FTIR. The impact of polymer concentrations on drug release and tensile strength was investigated using a 2^2 full factorial design (Design expert 13) (Table 1). To obtain an optimum batch, another ANOVA was performed.

Initially, the selected polymers, namely HPMC K100, Eudragit RS100, and PVP K30, were dissolved in a hydroalcoholic solvent system containing ethanol and water in a 70:30 ratio. The polymers were allowed to swell and form a homogeneous viscous solution under constant stirring. To this polymeric solution, glycerol, 15% of the total polymer weight was incorporated to impart flexibility and prevent brittleness of the final film. The optimized PCB NLC-Neusilin powder (equivalent to 172.5 mg PCB per patch area) was then dispersed uniformly into the polymeric mixture under continuous stirring, ensuring homogeneity. To boost the drug's skin penetration, oleic acid, a permeation enhancer, was added at a concentration of 3%. To get rid of trapped air bubbles, the finished mixture was degassed. The prepared dispersion was carefully cast onto a flat glass mould lined with a Polyethylene Terephthalate (PET) laminated sheet which served as the backing membrane. A homogeneous, flexible film was produced by drying the cast solution at 40°C in a hot air oven. Once dried, the film was peeled off and cut into circular patches of defined surface area of 40 cm^2), each containing the required dose of PCB. For reservoir-type patches, a thin layer of medical-grade Pressure-Sensitive Adhesive (PSA) was applied over the dried film to improve adherence to the skin surface.

Optimization of prepared transdermal patches

The concentrations of HPMC K100%w/v (X1) and Eudragit RS100%w/v (X2) were used as independent variables to optimize the manufactured batches. Tensile strength (Y2) and the amount of time needed for 90% drug release (Y1) are dependent variables.

Evaluation Of Optimized Batch: The optimized batch were evaluated for following parameters.[24-27]

Physicochemical Evaluation: The prepared PCB-NLC transdermal patches were subjected to physicochemical evaluation to ensure uniformity, flexibility, and suitability for transdermal application.

Thickness: Measured at five different points using a digital micrometer, and mean±SD values were calculated.

Weight variation: Individual patches (2 cm^2) were weighed using an analytical balance, and variation was recorded.

Folding endurance: Each patch was repeatedly folded at the same place until breakage or cracks appeared. The number of folds before breaking indicated flexibility.

Tensile strength: Determined using a modified weighing balance, expressed in kg/cm^2.

pH of surface: The pH of the patch's surface was measured using a calibrated digital pH meter after patches were soaked to swell in 1 mL of distilled water for 1 hr.

Drug content uniformity: Patches were cut into small pieces, dissolved in methanol, sonicated, and analyzed by UV spectrophotometry at λ_{max} of PCB max ≈ 266 nm).

Study of in vitro Release: A Franz diffusion cell with a dialysis membrane (molecular weight cutoff: 12-14 kDa) was used to measure the *in vitro* release of PCB from the improved NLC-based transdermal patches.[28] The diffusion cells' receptor tube was filled with 20 mL of Phosphate Buffer Saline (PBS, pH 7.4), kept at 37±0.5°C, and constantly agitated at 100 rpm to replicate physiological conditions. On the donor compartment of the diffusion cells with dialysis membrane, patches measuring 2 cm^2 in size (corresponding to a specific PCB dose) were placed. 1 mL sample were taken from the receptor medium at predetermined intervals (0, 2, 4, 8, 12, 24, 36, 48, and 72 hr), and sink conditions were maintained with an equal volume of fresh PBS. Pre-validated for linearity, precision, accuracy, and sensitivity, the samples were analyzed using established LOD and LOQ values of the HPLC-UV method (Table 2) operating at a λ of 266 nm with a C18 column and isocratic elution using acetonitrile: water 70:30 containing 0.1% formic acid to determine the cumulative percentage release of PCB. Kinetic models (zero-order, first-order, Higuchi, and Korsmeyer-Peppas) were fitted to the mechanism of drug release data.

Studies on *ex vivo* Skin Permeation and Skin Retention

Full-thickness goat skin was employed as a surrogate for human skin due to its comparable barrier properties. Fresh goat ears were procured from a local slaughter house. The tissue was thoroughly washed with normal saline, and hair was carefully trimmed with clippers, avoiding the use of shaving cream to prevent surface alterations. After carefully removing subcutaneous fat with a scalpel to produce clean skin sheets, PBS at pH 7.4 was equilibrated for 30 min.[29]

The thickness of the skin was maintained within the range of 1.5-2.0 mm, while selected samples were reduced to split-thickness (approximately 500-700 µm) using a dermatome for sensitivity analysis. Skin integrity was confirmed before mounting by measuring electrical resistance across the membrane, with values above 20 $k\Omega \cdot cm^2$ considered acceptable, or by assessing Trans-Epidermal Water Loss (TEWL), with acceptable values below 10 $g\ m^{-2}\ h^{-1}$.

Vertical Franz diffusion cells with an effective diffusion area of 2.0 cm^2 and a receptor volume of 20 mL were used for the permeation tests. With the stratum corneum facing the donor side, the skin was positioned between the donor and receptor compartments. The receptor medium consisted of PBS (pH 7.4) containing 20% v/v ethanol and 0.5% w/v Tween 80, which was revalidated to ensure that PCB solubility remained more than ten times higher than the maximum expected sample concentration, thereby maintaining sink conditions. To maintain the skin surface temperature at about 32°C, the receptor compartment was constantly agitated at 600 rpm and kept at 37±0.5°C.

For the test formulation, PCB loaded NLC transdermal patch discs of 2 cm^2 were used, with each disc containing PCB equivalent to 8 mg, standardized for *ex vivo* evaluation. The patches were gently affixed onto the stratum corneum surface and lightly occluded with a clip to prevent edge leakage. For comparison a free PCB solution prepared in a propylene glycol: ethanol: water mixture (40:30:30, v/v/v), applied as a finite dose of 50 µL per 2 cm^2. This solution was thermodynamically activity-matched to the PCB content in the patch extract and confirmed to be below saturation to avoid crystallization.

Samples were aliquoted from receptor medium at decided intervals of 0, 2, 4, 8, 12, 24, 36, 48, 60, and 72 hr. 1 mL of receptor fluid was extracted at each time interval, and sink conditions were consistently created using an equivalent volume of new medium. A validated HPLC-UV method was mainly used for PCB quantitative measurement (Table 1). Q(t) (µg cm^{-2}), the cumulative PCB penetration per unit area, was computed and adjusted for sampling. Using linear regression analysis, the steady-state flow (Jss) was calculated from the linear part of the permeation curve (usually between 8 and 48 hr), and the lag time (tL) was calculated from the x-intercept. The ratio of Jss for the

test patch to that of the control solution was used to compute the permeation Enhancement Ratio (ER). Analytical reliability was confirmed by mass balance analysis at the conclusion of the trial, which showed that the total of donor residue, drug retained in the skin, and receptor content accounted for 95-105% of the applied dose.

Additionally, a drug-free patch served as a blank control to ensure there was no analytical interference. For data comparison and reproducibility, results were expressed per cm^2.

Skin retention (post-permeation)

The donor preparations were carefully removed at the conclusion of the 72-hr permeation trial, and any loosely attached formulation was removed by cleaning the skin's surface three times with cotton swabs that had been mildly wet with PBS. The stratum corneum fraction was separated by tape stripping, wherein fifteen sequential adhesive strips (D-Squame®) were applied to the exposed area using a constant pressure roller with 10 sec of contact. The first strip was discarded, while strips 2-15 were pooled to represent the stratum corneum fraction. These were extracted in methanol: water (80:20) with the aid of vortex mixing and Filtration. After the tape was removed, the residual skin was heated in a water bath at 60°C for 60 sec to help separate the epidermis from the dermis, and it was then triturated to release the medicine that had been trapped. Both fractions underwent meticulous weighing, extraction in an 80:20 methanol:water ratio, and filtration via illipore TM filters. PCB content in the stratum corneum, epidermis, and dermis extracts was quantified using the validated HPLC-UV method. To provide a comprehensive picture of drug distribution across the layers, skin retention findings were expressed as both µg per gram of tissue and µg per cm^2 of application area.

Anti-cancer action *in vitro*

The National Centre for Cell Science (NCCS) in Pune provided the human breast cancer cell line MCF-7, which was kept in MEM medium enhanced with 10% fetal bovine serum. The cells were cultured for 24 hr at 37°C in a humidified environment with 5% CO_2 at a density of 1 × 10^ cells/mL. A 96-well tissue culture plate with 100 µL of culture media and 100 µL of water was filled with about 70 µL of the cell suspension.[30,31]

The corresponding wells were filled with test samples at concentrations between 10 and 100 µg/mL. Cell suspension and 0.2% DMSO made in PBS were added to control wells. In order to assess cell viability, all tests were carried out in triplicate using untreated control cells. The plates were kept in a CO_2 incubator (Thermo Scientific BB150) at 37°C for 24 hr.

Following incubation, each well received 20 µL of MTT reagent (5 mg/mL in PBS) after the culture media was properly removed. The plates were further incubated for 4 hr under the same conditions to allow formation of formazan crystals. The medium was then entirely discarded, and the crystals were dissolved by adding 200 µL of DMSO. The plates were further incubated at 37°C for 10 min while covered with aluminum foil. Lastly, an ELISA microplate reader (Benesphera E21) was used to measure the samples' absorbance at 570 nm.

Table 1: Batches of PCB-loaded transdermal patches using 2^2 full factorial design.

Formulations	F1	F2	F3	F4
HPMC K100% w/v	15	10	10	15
Eudragit RS100% w/v	10	5	10	5
PCB NLC loaded Neusilin powder	Equivalent to 172.5 mg PCB/patch of 40 cm^2	Equivalent to 172.5 mg PCB/patch of 40 cm^2	Equivalent to 172.5 mg PCB/patch of 40 cm^2	Equivalent to 172.5 mg PCB/patch of 40 cm^2
PVP K30% w/v	1	1	1	1
Glycerol % w/v	15	15	15	15
Oleic acid % w/v	3	3	3	3
Ethanol:Water, 70:30)	Qs	qs	Qs	qs

Table 2: Linearity data of PCB.

Concentration µg/mL	Peak area			Average peak area	SD	%RSD
	1	2	3			
30	985.866	974.606	964.34	974.9373	±8.79	0.90
60	1932.517	1974.103	1945.868	1950.829	±17.33	0.88
90	3033.856	3051.149	3018.681	3034.562	±13.26	0.43
120	4070.611	4224.95	4117.901	4137.821	±64.56	1.56
150	5212.646	5204.875	5215.736	5211.086	±4.56	0.08

Stability Studies

In compliance with ICH Q1A (R^2) criteria, a stability study of the optimized Palbo-NLC transdermal patch was conducted. The prepared patches were placed in aluminum foil-laminated pouches and kept in a stability room with accelerated stability conditions at 40±2°C and 75±5% relative humidity. Samples were assessed at predefined intervals of 0, 1, 2, and 3 months during the course of the three-month trial.[32,33]

At each sampling interval, the patches were examined for various physicochemical and mechanical characteristics, including physical appearance such as color, brittleness, flexibility, and any evidence of phase separation. In addition, patch thickness, weight uniformity, and drug content (%) were determined. Using a Franz diffusion cell, the *in vitro* drug release profile was evaluated for 72 hr. To ascertain the stability and integrity of the formulation during storage, mechanical characteristics such as tensile strength and folding endurance were also assessed.

RESULTS

HPLC Analytical technique development

Using a C18 column and isocratic elution with acetonitrile: water 70:30 containing 0.1% formic acid, samples with concentrations between 30 and 150 µg/mL in methanol were examined at the detection wavelength of 266 nm. Linearity was evaluated across the concentration levels, resulting in a linear equation of y=35.531x - 135.94 (correlation coefficient R^2= 0.999) demonstrating strong linearity. Additionally, the %RSD values were within the acceptable range, as presented in Table 2.[18]

Compatibility studies of selected polymers with PCB by FTIR: All the selected polymers and excipients as per pharmacotechnical, biopharmaceutical, and regulatory considerations were found to be compatible with PCB by FTIR (Figure 1).

Determination of quantity of PCB-NLC to be loaded in a patch: Since for very first-time transdermal route for PCB-NLCs are investigated in this study, to estimate how much drug must reach the systemic circulation; specifically on the site of action per day the clinical oral dose and oral bioavailability of PCB was considered.

Oral dose of PCB is 125 mg once daily and mean absolute oral bioavailability ≈ 46%, so a 125 mg oral dose gives ~57-58 mg systemic exposure/day (125 mg × 0.46 ≈ 57.5 mg/day). The transdermal route was selected for site specific drug delivery of the drug for longer period (~72 hr). Thus, considered approximately 25% of total bioavailable drug reaches site of action. (Taking into account its high protein binding, BCS II properties, PK/PD and safety etc.).

For 72 hr, equivalent systemic delivery ≈ 172.5 mg/72 hr and 25% of systemic drug=43.125 mg/72 hr, on site of action).

Required Flux calculation for a 72 hr patch=Jreq=(Total delivered in 72 hr (mg))/ (Patch area (cm^2) ×72 hr).

$$J_{req} = 43.125mg/(40c\,m^2 \times 72hr) = 14.97\mu g/c\,m^2/hr$$

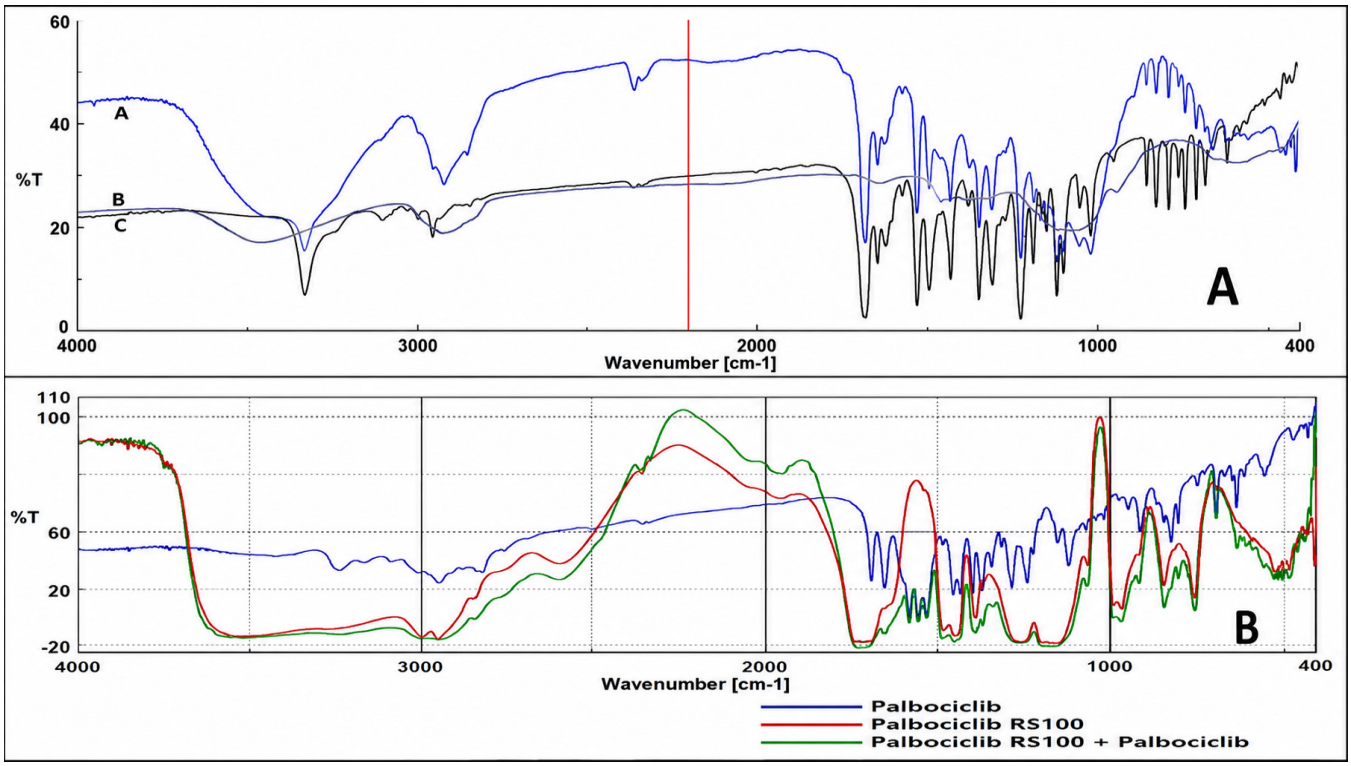

Figure 1: Compatibility studies of A. HPMC K100 with PCB by FTIR (A) PCB with HPMC K100 (B) PCB (C) HPMC K100 and B. Compatibility studies of Eudragit RS100 with PCB by FTIR.

$$\text{Totaldelivered} = 43.1\text{mg} \div 40\text{c}\,\text{m}^2 = 1.078\text{mg/c}\,\text{m}^2\,\text{over72hr}$$

Required loading per cm^2 (since only 25% fraction 'f' reaches target): 1.078/0.25= 4.3125mg/cm^2

$$\text{Totalpatchcontent} = 4.3125\ \text{mg/c}\,\text{m}^2 = 4.3125 \times 40\text{c}\,\text{m}^2 = 172.5\ \text{mgtoachieve}\,J_{req}.$$

172.5 mg of PCB required per patch of 40 cm^2.

The ratio of Neusilin US2 with PCB-NLCs=1.5:1=450 mg Neusilin US2: 300 mg PCB-NLCs=450 mg Neusilin US2: 30 mg PCB drug.

For 172.5 mg of PCB 2578.5 mg (2.5785 g of Neusilin US2) was taken and patches were prepared by solvent casting method (Figure 2).

Evaluation of prepared batches

In vitro drug release studies: The prepared batches were shown 90% cumulative drug release for 48 to 84 hr (Table 3).

Tensile strength: It indicates the ability of the patch to withstand pulling force without breaking. Prepared batches showed tensile strength (N*mm^2) in range of 1.8-4.5 N*mm^2 (Table 3). Very high tensile strength patch may become rigid and less flexible Very low tensile strength patch may tear easily.

Effect of variable on Time required for 90% drug release

$$\text{Timerequiredfor90\%drugrelease}\ (Y1) = 66 + 6.00 \times X1 + 12 \times X2$$

The positive coefficients of both X1 (+6.00) and X2 (+12.0) indicate that increasing either polymer concentration increases the time required for 90% drug release. The higher coefficient of Eudragit RS100 (+12) compared to HPMC K100 (+6) shows that Eudragit RS100 has a stronger retarding effect on drug release than HPMC K100.

The Half normal plot and Pareto plot (Figure 3) confirming that as the levels of both polymers increase, the time required for drug release significantly increases. No interaction term (X1X2) appears in the equation, suggesting that the combined effect of both polymers is additive rather than synergistic or antagonistic.

Effect of variables on tensile strength

$$\text{Tensilestrength}(Y2) = +2.95 + 0.050X1 + 0.65X2 - 0.45X1X2$$

The ANOVA results for tensile strength indicated that both HPMC K100 (X1) and Eudragit RS100 (X2) had a positive influence on the response (Tensile strength), with Eudragit RS100 showing a more pronounced effect (coefficient +0.65) compared to HPMC K100 (+0.050). The regression model suggested a significant negative interaction between the two polymers (-0.45), indicating that at higher concentrations, their combined effect reduced tensile strength instead of producing an additive increase.

Half normal plot and Pareto plot (Figure 3) confirmed that tensile strength improved predominantly with increasing Eudragit RS100, while HPMC K100 contributed only marginally. Thus, Eudragit RS100 was identified as the key determinant of patch mechanical strength, whereas excessive combinations of both polymers could compromise film integrity. Interaction Term (-0.45 X1X2) the negative coefficient suggests an antagonistic interaction between HPMC K100 and Eudragit RS100. At higher concentrations of both polymers, tensile strength decreases slightly instead of increasing additively. This may be due to reduced polymer miscibility or phase separation when both are high.

By employing optimization criteria such as minimum concentration of HPMC 100K, maximum concentration of Eudragit RS100, maximum time required to 90% and tensile strength the software suggested F3 as optimized batch. The batch further characterized as per specified in Table 4.

Figure 2: Trial batches of PCB NLCs -loaded transdermal patches by solvent casting.

Table 3: Observed Results for Critical Process Parameters Cumulative % drug release and tensile strength of Trial batches of PCB -loaded transdermal patches for ANOVA.

Cumulative % drug release				
Time (hr)	**F1**	**F2**	**F3**	**F4**
0	0	0	0	0
2	4.20±2.5	12.12±2.1	8.50±3.6	9.02±0.9
4	7.36±1.9	19.50±1.8	15.60±1.2	15.42±3.2
8	10.50±2.1	28.04 ±2.6	28.4±2.5	29.95±3.6
12	15.80±1.5	38.99 ±1.8	39.7±2.3	41.95±2.3
24	30.40±3.8	78.94 ±1.4	58.9±4.1	65.85±1.6
36	50.80±2.9	90.22 ±2.0	67.3±3.2	76.58±2.3
48	61.70±1.9	99.99 ±0.1	75.4±1.2	82.52±5.1
60	75.80±0.9		83.6±3.1	91.50±1.3
72	83.44±1.2		90.2±2.2	98.25±2.1
84	90.25±3.7		95.6±4.0	
Observations of tensile strength of prepared transdermal patches				
Tensile strength (N*mm$^{2)}$	3.2±1.55	1.8±1.02	4.5±3.33	2.8±1.08

In vitro drug Release kinetics studies

The optimized PCB-loaded NLC transdermal patch (F3) exhibited a sustained drug release over 72 hr (Table 3). An initial slow release of ~40% was observed within the first 12 hr, likely due to diffusion of surface-associated drug from the lipid matrix, followed by a controlled release phase reaching ~90% cumulative release at 72 hr. This sustained profile indicates efficient drug encapsulation within the NLC lipid matrix and gradual diffusion through the polymeric patch. A diffusion-controlled mechanism was confirmed by release kinetics, which best fit the Higuchi model (R^2>0.98). The Korsmeyer-Peppas model revealed non-Fickian diffusion (0.45 <*n*<0.89), indicating that the prolonged release was caused by both drug diffusion and polymer relaxation.

The extended release of PCB up to 72 hr is highly advantageous in a transdermal system, as it can reduce the frequency of administration and maintain a consistent plasma concentration at site of administration.

Studies on *ex vivo* Skin Permeation and Skin Retention

Permeation profile and kinetic parameters

The PCB-NLC patch and the free PCB solution showed a distinct difference over a 72-hr period in the *ex vivo* cumulative permeation study of PCB via goat skin (Figure 4). From the early phase, the patch showed superior permeation, with 38.4 µg cm^{-2} at 2 hr compared to 22.6 µg cm^{-2} for the free solution. This advantage continued to widen with time, and by 24 hr, the patch had delivered 372.6 µg cm^{-2}, nearly 1.75 times higher than the free solution (212.4 µg cm^{-2}). In the mid-to-late phase, the patch maintained sustained release, reaching 608.9 µg cm^{-2} at 48 hr, approximately double the value of the free solution (304.7 µg cm^{-2}). By 72 hr, the cumulative permeation from the patch was 742.3 µg cm^{-2}, more than twice that of the free solution (321.5 µg cm^{-2}). These results align with kinetic parameters, where the patch exhibited a higher steady-state flux Jss 14.8±1.2 µg cm^{-2} h^{-1}, shorter lag time 2.9±0.4 tLt (h), and an enhancement ratio of around 2.4 compared to the free drug. (Jss 6.2±0.7 µg cm^{-2} h^{-1}, Lag time, tLt (h) 4.6±0.5). Overall, the PCB-NLC patch significantly improved both the rate and extent of drug permeation, offering faster onset, prolonged delivery, and enhanced bioavailability compared to the conventional solution.

The PCB NLC patch produced a ~2.4-fold higher flux and a significantly shorter lag time than free PCB solution. The receptor profiles showed a near-linear region from ~8-48 hr for both groups, consistent with diffusion-controlled transport. The higher Jss is attributed to oleic acid mediated lipid extraction/fluidization of SC lipids, nano sized NLCs enhancing partitioning into the SC, and sustained release from the polymeric matrix maintaining a higher thermodynamic activity at the skin interface. Mass balance recoveries were within acceptance (95-105%), supporting analytical robustness.

Kinetic fitting (not tabulated) showed the cumulative profile vs. √time exhibited excellent linearity (R^2>0.98) for the patch group over the main window, indicating Higuchi-type diffusion across the membrane coherent with *in vitro* release. The reduced lag time suggests faster initial barrier saturation by enhancer-assisted NLCs.

Skin retention study

The patch achieved ~3.1× higher total skin retention vs. free PCB solution (Stratum corneum (tapes 2-15) 112.6±12.1 µg cm^{-2}, Epidermis 126.9±15.4 µg cm^{-2}, Dermis 153.7±17.8 µg cm^{-2}) compare with free PCB solution (Stratum corneum (tapes 2-15) 34.7±6.8 µg cm^{-2}, Epidermis 41.5±7.9 µg cm^{-2}, Dermis 50.4±9.6). With pronounced deposition in epidermis and upper dermis desirable for localization near breast tissue and potential reduction of systemic. Elevated SC loading likely acts as a drug reservoir, supporting the sustained receptor permeation observed. The blank patch showed no detectable PCB, confirming specificity.

In vitro anti-cancer activity

PCB NLCs are shown in Sample F1, and transdermal patches loaded with PCB NLCs are shown in Sample F2 (Figure 5).

The cytotoxic effects of samples F1 and F2 were evaluated against MCF-7 using the MTT assay. Samples F1 and F2 showed a dose-dependent decline in cell viability, suggesting that greater doses had more cytotoxic effects. Cell viability decreased from 93.60% to 58.51% in PCB-SD sample F1, indicating significant cytotoxicity. Sample F2 (PCB NLC-TP) exhibited more severe cytotoxic effects than sample F1 (PCB-NLCs), with cell viability declining from 87.34%.

Sample F1 (PCB-NLCs): At lower concentrations, the cell viability was 92.80%, meaning only a small number of cells were affected. At higher concentrations, the cell viability dropped to 68.51%, showing increased cytotoxicity. This demonstrates that the both PCB-NLC and PCB NLC-TP can kill cancer cells, but its effectiveness of (PCB NLC) is limited compared to the PCB NLC-TP.

Sample F2 (PCB NLC-TP): Cell viability started at 95.34% at lower concentrations, which is already slightly lower than F1, suggesting better initial cytotoxicity. The text implies that at higher concentrations, the reduction in cell viability was even greater than F1 up to 66.63%. This suggests that the nanoparticle

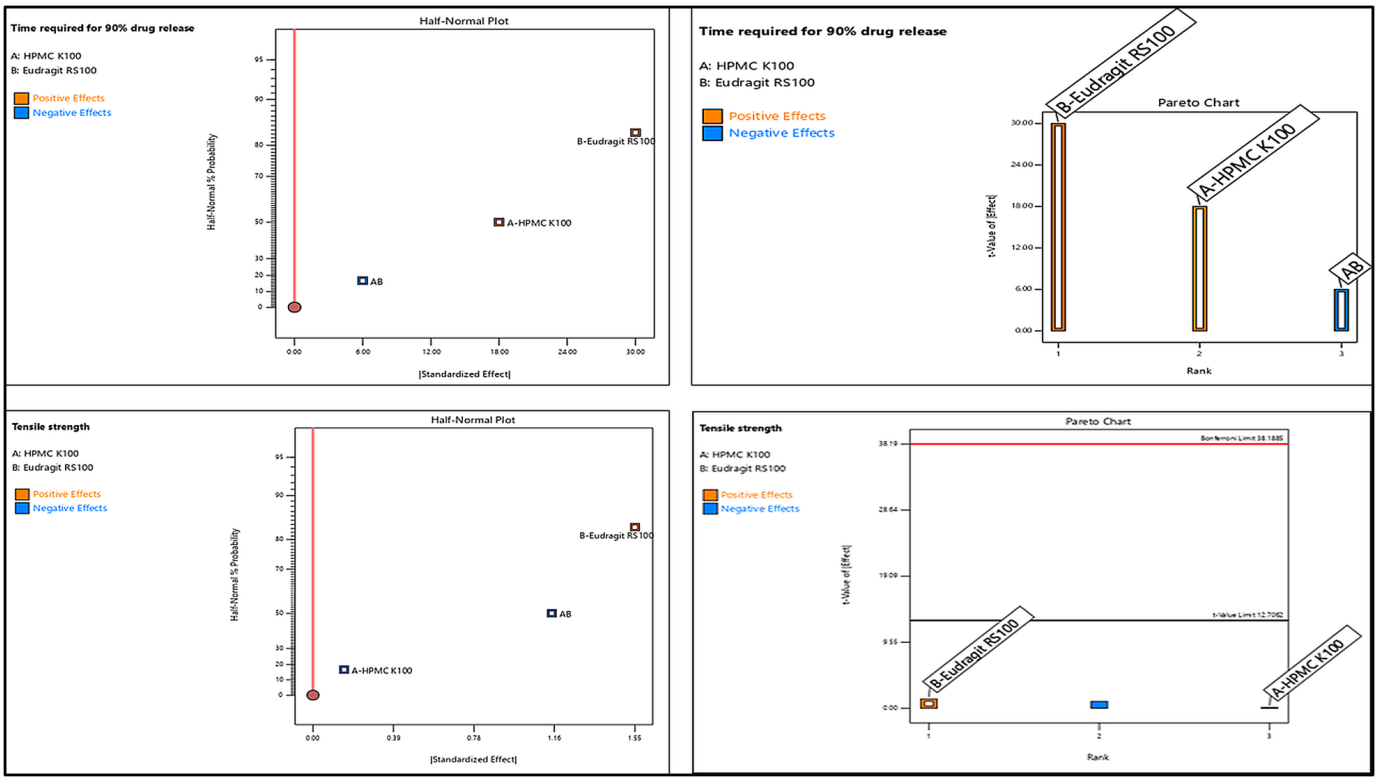

Figure 3: Half normal plot and Pareto plot of Time required for 90% drug release and Tensile strength.

Table 4: Physicochemical Evaluation of Batch F3 PCB-NLC Transdermal Patches.

Parameter	Mean Value±SD (*n*=3)		Acceptable Range
Thickness (mm)	0.198	±0.012	0.15 - 0.25 mm
Weight variation (mg/2 cm^2)	95.4	±2.8	±5% of mean
Folding endurance	32	±15	>30 (Good)
Tensile strength (kg/cm^2)	4.5	±0.17	>2.5 (Good)
Surface pH	6.48	±0.21	5.5 - 7.0 (Skin-friendly)
Drug content uniformity (% of theoretical)	96.8	±1.9	90-110%

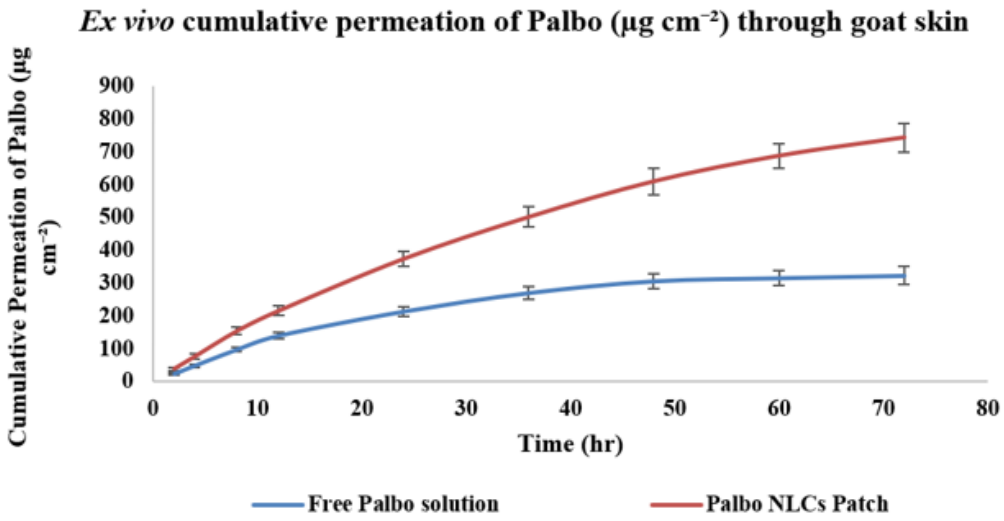

Figure 4: *Ex vivo* cumulative permeation of PCB (µg cm^{-2}) through goat skin.

formulation (PCB NLC-TP) enhanced the drug's cytotoxic effect, likely due to better drug delivery, improved cellular uptake, or sustained release.

Stability study

The stability study confirmed that the optimized PCB-NLC transdermal patch was stable under accelerated conditions for 3 months.

Physical integrity was maintained, with patches remaining flexible, transparent, and free of cracks or crystallization. Only a slight reduction in glossiness was observed at 2 months, which did not affect performance. Thickness, weight uniformity, and surface pH remained consistent, indicating no significant moisture uptake or polymer degradation. Mechanical strength (folding endurance and tensile strength) showed only a marginal decline, suggesting that the polymer matrix retained adequate flexibility and durability throughout the storage period. The drug content stayed over 96%, indicating that PCB degradation during storage was minimal. Due to modest variations in polymer hydration, the *in vitro* release profile showed only a slight drop (~2% over 3 months), but it was still within acceptable bounds.

DISCUSSION

The above said study aims to develop and optimize transdermal patch embedded with PCB-NLCs. The previously optimized NLCs formulation of PCB[18] was developed using a Box-Behnken design through microemulsion followed by ultra-sonication. In the formulation a surfactant blend of Span 80 and Tween 80 in 4.44:1 ratio was selected using a green approach (calculating theoretically require HLB of formulation) for PCB delivery. The optimized batch showed a particle size of 165 nm, PDI of 0.3, zeta potential around -34 mV, entrapment efficiency above 98%, and drug loading of 9.9%. DSC and XRD studies confirmed reduced crystallinity and successful incorporation of PCB into the amorphous lipid matrix, while TEM analysis revealed spherical nanosized particles with smooth surfaces. *In vitro* release studies demonstrated sustained drug release for 10 hr. Cytotoxicity studies on MCF-7 cells showed enhanced anticancer activity of PCB-loaded NLCs compared with the free drug, likely due to improved cellular uptake and retention. Overall, Sterotex HM and Captex 300 based PCB NLCs stabilized with Span 80 and Tween 80 demonstrated strong potential for development of transdermal patch.

The selection of ingredients for the transdermal patch was based on pharmacotechnical, biopharmaceutical, and regulatory considerations. PCB is suitable for transdermal delivery due to its acceptable molecular weight, moderate lipophilicity (log P ≈ 1), and low daily dose requirement, enabling effective permeation across the stratum corneum as per pharmacopeial guidelines. HPMC 100K and Eudragit RS100 were chosen as matrix-forming polymers owing to their film-forming ability, mechanical strength, compatibility, and controlled-release characteristics, while glycerol was incorporated as a plasticizer to improve flexibility and prevent brittleness. Oleic acid was selected as a penetration enhancer to transiently reduce skin resistance and enhance drug flux.[34] Additionally, oleic acid has been reported to promote de-adsorption of lipidic or drug-loaded formulations from Neusilin® by penetrating its mesoporous structure and displacing adsorbed molecules, thereby increasing elution and influencing *in vitro* release behavior.[35]

Among the selected excipients, HPMC 100K and Eudragit RS100 had the greatest influence on drug release and tensile strength. HPMC 100K forms a hydrated gel layer that controls release by diffusion and polymer relaxation, with increasing concentrations producing a thicker gel barrier and slower release. Eudragit RS100, a water-insoluble but permeable polymer, retards release

by reducing water uptake, increasing matrix tortuosity, and minimizing burst release, while also enhancing mechanical strength.[23]Based on their individual and combined effects, HPMC K100 (10-15% w/w) and Eudragit RS100 (5-10% w/w) were selected. The combination allowed HPMC K100 to act as the primary release-controlling polymer, while Eudragit RS100 fine-tuned sustained release and improved patch integrity.

Half normal plot and Pareto plot showing Eudragit RS100 is most impactful factor for both drug release and tensile strength. However, the polynomial equation indicating drug release was significantly extended by rising both polymer concentrations. The absence of an interaction term (X_1X_2) advises an additive, rather than synergistic or antagonistic, effect. In contrast, the equation for tensile strength established that mechanical strength increased mainly with higher Eudragit RS100 levels, while HPMC had a minimal contribution. Patch strength was therefore frequently determined by Eudragit RS100, while high concentrations of both polymers could compromise film integrity. The opposed relationship between HPMC and Eudragit RS100 is indicated by the negative interaction term ($-0.45X_1X_2$). High concentrations of both lead to a modest decrease in tensile strength, which is possibly caused by phase separation or decreased polymer miscibility.

Over a 72-hr period, the enhanced NLC-loaded transdermal patch demonstrated continuous PCB release *in vitro*. Diffusion of the surface linked drug was probably responsible for the initial slow release of around 40% over the first 12 hr. This was followed by a controlled release phase (Higuchi model) that reached about 90% cumulative release at 72 hr. This outline shows slow diffusion through the polymeric patch and effective drug encapsulation within the NLC lipid matrix.

PCB- NLC patch attained a ~2.4-fold greater flux and a considerably shorter lag time than free Palbo solution, according to an *ex vivo* drug release study. For both groups, the receptor profile displayed near-linear permeation between 8 and 48 hr, which is consistent with diffusion-controlled transport. The increased steady-state flux was ascribed to sustained drug release from the polymeric matrix, improved partitioning of nanosized NLCs, and stratum corneum lipid fluidization mediated by oleic acid. Analytical reliability was validated by mass balance recoveries (95-105%). Excellent linearity of cumulative release vs √time (R^2>0.98) was shown by kinetic analysis, suggesting faster barrier saturation by enhancer-assisted NLCs and indicating Higuchi-type diffusion.

The patch presented ~2.4-fold higher skin retention than free Palbo solution, with improved deposition in the epidermis and upper dermis, preferring localized delivery and reduced systemic exposure. Increased stratum corneum loading possibly served as a drug reservoir supporting sustained permeation,[36,37] while the blank patch presented no detectable PCB, confirming specificity. MTT assay results of PCB-NLC embedded transdermal patch shows good of cyto toxic activity on MCF-7 cell line. The improved initial cytotoxicity of the PCB-NLC-loaded patch (F2) compared to that of PCB-NLCs alone (F1) can be attributed to the

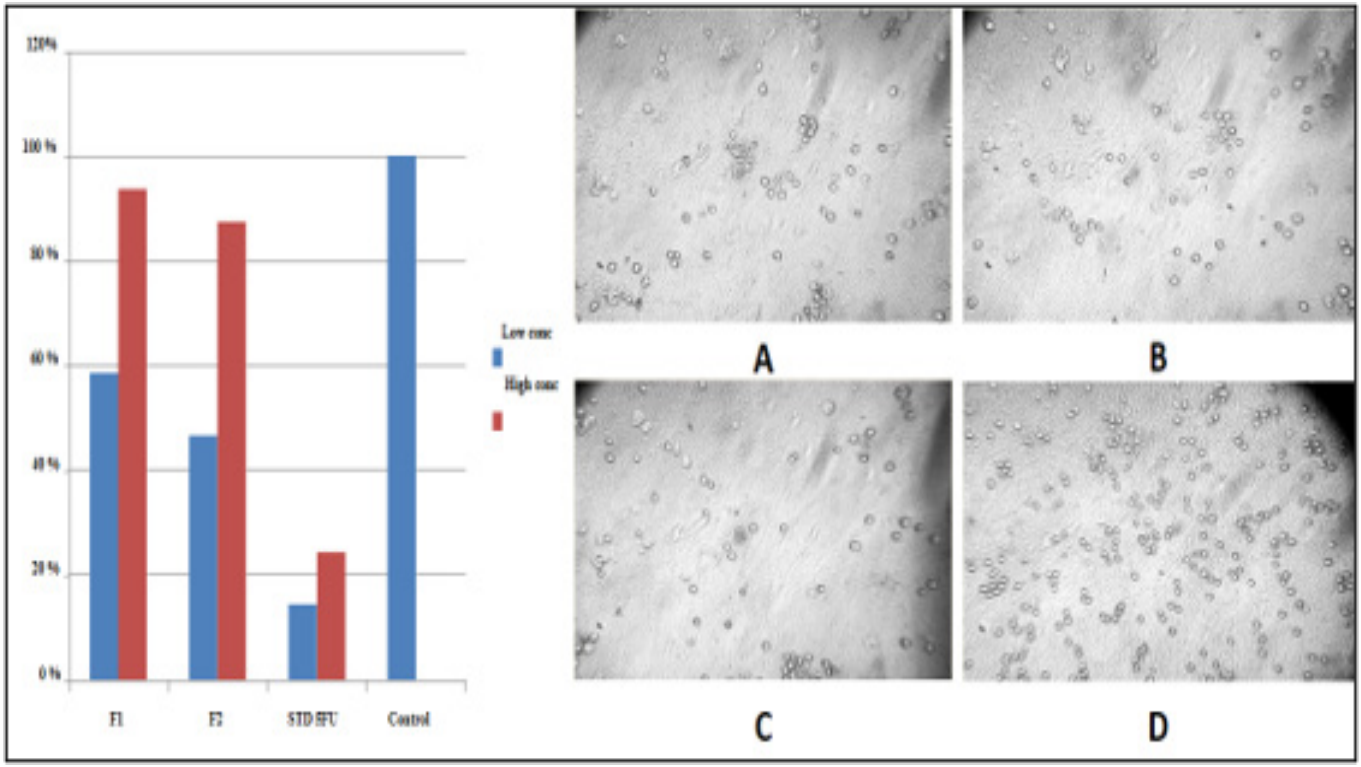

Figure 5: Comparison of % Cell Viability in MTT assay MCF-7 Cells (F1 PCB- NLCs vs F2 PCB -NLCs loaded transdermal patch and Standard 5FU) and MTT assay results of A) PCB-SD B) PCB -NLCs C) Standard 5-FU D) Control.

enhanced cellular uptake and intracellular accumulation of PCB by the lipid-based nanocarrier system. Furthermore, the oleic acid present in the patch can increase the membrane fluidity, thus favoring a higher interaction of drug-loaded nanoparticles with MCF-7 cells and resulting in enhanced early cytotoxic effects.[38] Accelerated stability study indicates no significant changes in the physical and chemical properties of prepared patch specify that the optimized formulation possesses satisfactory stability and can maintain its physicochemical performance during storage under accelerated conditions.

CONCLUSION

A transdermal patch loaded with PCB-NLCs was effectively created, displaying prolonged release from the HPMC/Eudragit polymeric matrix and enhanced and regulated drug penetration due to the synergistic effect of oleic acid and lipid-based NLCs. The formulation supported continued drug availability over 72 hr by keeping a constant concentration gradient throughout the skin, which increased steady-state flow and led to the establishment of a sizable in-skin drug depot spanning the stratum corneum, epidermis, and dermis. Despite better penetration and a shorter lag time, low receptor phase drug levels comparative to the given dose establish that systemic exposure remained under control. Additionally, proper mass balance and the absence of phase separation or crystallization established the patch's stability and endurance during wear. MTT assay results ensure retaining of anti-cancer action of PCB-NLC embedded transdermal patch. These conclusions highlight the possibility of the recommended approach as a viable transdermal administration route for Palbociclib, reassuring more IVIVC and *in vivo* studies.

ACKNOWLEDGEMENT

The author sincerely acknowledges Dr. Shivajirao Kadam College of Pharmacy, K. Digraj; Bharati College of Pharmacy, Kolhapur; and Biocyte Institute of Research and Development, Sangli, for providing the necessary premises, laboratory facilities, and equipment to carry out the present research work.

ABBREVIATIONS

PCB: Palbociclib; **NLC:** Nanostructured lipid carrier; **HPMC:** Hydroxypropyl Methylcellulose; **PVP:** Polyvinylpyrrolidone; **FTIR:** Fourier Transform Infrared Spectroscopy; **RP-HPLC:** Reverse Phase High Performance Liquid Chromatography; **ICH:** International Council for Harmonisation; **OD:** Once Daily; **BCS:** Biopharmaceutics Classification System; **PK/PD:** Pharmacokinetic/Pharmacodynamic; **HLB:** Hydrophilic-Lipophilic Balance; **DSC:** Differential Scanning Calorimetry; **XRD:** X-ray Diffraction; **TEM:** Transmission Electron Microscopy; **PDI:** Polydispersity Index; **Jss:** Steady-state flux; **ER:** Enhancement ratio; **SC:** Stratum Corneum; **TEWL:** Trans-epidermal water loss; **MTT:** 3-(4,5-dimethylthiazol-2-yl)-2,5-diphenyltetrazolium bromide; **DMSO:** Dimethyl Sulfoxide; **MEM:** Minimum Essential Medium; FBS: Fetal Bovine Serum; PBS: Phosphate Buffer Saline; **RSD:** Relative Standard Deviation; **LOD:** Limit of Detection; **LOQ:** Limit of Quantitation; UV: Ultraviolet; **PET:** Polyethylene Terephthalate; PSA: Pressure-Sensitive Adhesive; **ANOVA:** Analysis of Variance; **IVIVC:** *In vitro-in vivo* correlation.

CONFLICT OF INTEREST

The authors declare that there is no conflict of interest.

AUTHORS CONTRIBUTION

The author N. Gurav carried out the experimental work, data analysis, and manuscript drafting. The co-authors A. Shinde and H. More contributed to study supervision, interpretation of results, critical review of the manuscript, and approval of the final version.

SUMMARY

An optimized Palbociclib loaded NLC transdermal patch was successfully prepared by using HPMC K100 and Eudragit RS100 polymers. The formulation showed good nanoparticle characteristics, sustained drug release for 72 hr, improved skin permeation (~2.4-fold higher flux), higher skin retention, enhanced cytotoxicity against MCF-7 cells and good mechanical properties. The *ex vivo, in vitro* and stability studies established its potential as a stable and effective transdermal delivery system for breast cancer therapy.

REFERENCES

1. Al-Zahrani NS, Patel AA, El-Gamal B, Ellatif MA, Nasif KA, Abd Elrouf MB, *et al.* Drug Repurposing Revealed Abemaciclib and Palbociclib as Inhibitor of Phosphodiesterase-5 (PDE5) in Cancer-Associated Fibroblasts Paving the Way for the Treatment of Breast Cancer. Ind J Pharm Edu Res. 2025;59(3):1221-30. doi:10.5530/ijper.20251022
2. Beaver JA, Amiri-Kordestani L, Charlab R, Chen W, Palmby T, Tilley A, *et al.* FDA Approval: Palbociclib for the Treatment of Postmenopausal Patients with Estrogen Receptor-Positive, HER2-Negative Metastatic Breast Cancer. Clinical Cancer Research. 2015;21(21):4760-6. doi:10.1158/1078-0432.CCR-15-1185
3. Shanabag A, Armand J, Son E, Yang HW. Targeting CDK4/6 in breast cancer. Exp Mol Med. 2025;57(2):312-22. doi:10.1038/s12276-025-01395-3
4. Sreenath ND, Pandalanghat S, Kapoor A, Govind R, Kaushik MR, Nair R, *et al.* A comparative analysis of Palbociclib and Ribociclib in metastatic hormone receptor-positive, HER2-negative breast cancer: a prospective mid term follow-Up study from an Indian cohort. BMC Cancer. 2025;25(1):1337. doi:10.1186/s12885-025-14270-1
5. Radosa JC, Cobo SLT, Dzieran J, Glastetter E, Chen C, Lingohr-Smith M, *et al.* Palbociclib treatment in patients with HR+/HER2- advanced or metastatic breast cancer and visceral metastasis: A systematic literature review. The Breast. 2025;84:104569. doi:10.1016/j.breast.2025.104569
6. Serra F, Lapidari P, Quaquarini E, Tagliaferri B, Sottotetti F, Palumbo R. Palbociclib in metastatic breast cancer: current evidence and real-life data. DIC. 2019;8:1-16. doi:10.7573/dic.212579
7. Tian X, Chen L, Chen Y, Zhang N. Adverse event profiles of CDK4/6 inhibitors: a disproportionality analysis of the FDA Adverse Event Reporting System (FAERS) database. Expert Opinion on Drug Safety. 2026;25(7):1329-39.doi:10.1080/14740338.2025.2465852
8. Park D, Varda M, Yeremian S, Hwang A, Huang C. CDK4/6 Inhibition in the Management of Metastatic HR+/HER2+ Breast Cancer: Systematic Review and Meta-analysis. Targ Oncol. 2026;21(1):13-21. doi:10.1007/s11523-025-01195-9

9. Zhou J, Lin X, Wang S, Xie M, Hu X, Cai J. Toxicity profiles of cyclin-dependent kinase 4/6 inhibitors: safety analysis from clinical trials and the FDA adverse event reporting system. Front Oncol. 2025;15:1673284. doi:10.3389/fonc.2025.1673284.
10. Bai W, Shi S, Yin D, Guo C, Song H, Hu Y, Gao J, Qiu B, Zhang X, Bi L, Wu H, Dong Z. Bioequivalence of a single dose of two palbociclib formulations in healthy Chinese subjects under fasting conditions: a two-period crossover study with rabeprazole pre-treatment. Front Pharmacol. 2025;16:1722151. doi:10.3389/fphar.2025.1722151.
11. Peruzzi E, Posocco B, Gerratana L, Nuti M, Orleni M, Gagno S, De Mattia E, Puglisi F, Cecchin E, Toffoli G, Roncato R. Exploring pharmacokinetic variability of palbociclib in HR+/HER2- metastatic breast cancer: a focus on age, renal function, and drug-gene interactions. Front Pharmacol. 2024;15:1420174. doi:10.3389/fphar.2024.1420174.
12. Gurav NH, Jadhav SA, Mudgal VD, Utage AC, Shinde AJ. Design and characterization of palbociclib loaded nano structured lipid carriers for treatment of breast cancer. J Comput Anal Appl. 2024;33(6):2668-2685. doi:10.48047/jocaaa.2024.33.06.101.
13. Kanp T, Dhuri A, Aalhate M, Manoharan B, Rode K, Munagalasetty S, *et al.* Investigation of a Palbociclib and Naringin Co-Amorphous System to Ameliorate Anticancer Potential: Insights on *in silico Modeling*, Physicochemical Characterization, *ex vivo* Permeation, and *in vitro* Efficacy. Mol Pharmaceutics. 2025;22(5):2446-65. doi:10.1021/acs.molpharmaceut.4c01224
14. Duan C, Liu W, Tao Y, Liang F, Chen Y, Xiao X, *et al.* Two Novel Palbociclib-Resorcinol and Palbociclib-Orcinol Cocrystals with Enhanced Solubility and Dissolution Rate. Pharmaceutics. 2021;14(1):23. doi:10.3390/pharmaceutics14010023
15. Hoque N, Choudhury A. Formulation Design, Optimization, and *in vitro* Evaluation of Palbociclib-Loaded Polymeric Nanoparticles. ASSAY and Drug Development Technologies. 2026;24(4):296-311. doi:10.1177/1540658X261429246
16. Kurawattimath V, Wilson B, Geetha KM, Divekar K. Surface functionalized albumin nanoparticles of palbociclib with amplified brain delivery for treating brain glioblastoma. Sci Rep. 2025;15(1):28433. doi:10.1038/s41598-025-13721-w
17. Cheng Z, Huang H, Yin M, Liu H. Applications of liposomes and lipid nanoparticles in cancer therapy: current advances and prospects. Exp Hematol Oncol. 2025;14(1):11. doi:10.1186/s40164-025-00602-1
18. Gurav NH, Jadhav SA, Mudgal VD, Utage AC. Design and characterization of palbociclib loaded nano structured lipid carriers for treatment of breast cancer. 2024;33(6).
19. Nehal N, Unnithan D, Emad NA, Aashish, Sartaj A, Baboota S, *et al.* Development and Preclinical Assessment of a Palbociclib Nanostructured Lipid Carrier for Potential Breast Cancer Management. Mol Pharmaceutics. 2025;22(3):1419-36. doi:10.1021/acs.molpharmaceut.4c01122
20. Hassanzadeh P, Arbabi E, Rostami F. Lipid-based nanocarriers provide prolonged anticancer activity for palbociclib: *in vitro* and *in vivo* evaluations. Acta Med Iran. 2021;59(6). doi:10.18502/acta.v59i6.6891.
21. Khade P, Gupta U, Kumar R, Mehra NK, Singh PK. Mucoadhesive Carbohydrate-Based Polymeric Nanocapsule Loaded with Palbociclib for Enhanced GIT Retention and *in vitro* Anticancer Efficacy in MDA-MB-231 Cells. AAPS PharmSciTech. 2025;27(1):32. doi:10.1208/s12249-025-03263-9 PubMed PMID: 41239020.
22. Zerang N, Mirjafary Z, Saeidian H, Rouhani M. Enhancing palbociclib efficacy with low toxicity in breast cancer using polycaprolactone-based nanocarriers. Results Chem. 2025;15:102283. doi:10.1016/j.rechem.2025.102283.
23. Nyamweya N, Hoag SW. Assessment of Polymer-Polymer Interactions in Blends of HPMC and Film Forming Polymers by Modulated Temperature Differential Scanning Calorimetry. Pharm Res. 2000;17(5):625-31. doi:10.1023/A:1007585403781
24. Bácskay I, Hosszú Z, Budai I, Ujhelyi Z, Fehér P, Kósa D, *et al.* Formulation and Evaluation of Transdermal Patches Containing BGP-15. Pharmaceutics. 2023;16(1):36. doi:10.3390/pharmaceutics16010036
25. Arunprasert K, Pornpitchanarong C, Piemvuthi C, Siraprapapornsakul S, Sripeangchan S, Lertsrimongkol O, Opanasopit P, Patrojanasophon P. Nanostructured lipid carrier-embedded polyacrylic acid transdermal patches for improved transdermal delivery of capsaicin. Eur J Pharm Sci. 2022;173:106169. doi:10.1016/j.ejps.2022.106169.
26. Rani M, Rohilla S, Sharma S, Chadda T. Optimization and Characterization of Lisinopril Loaded Transdermal Patches by Using Factorial Design. Ind J Pharm Edu Res. 2026;60(3):985-98. doi:10.5530/ijper.20261604
27. Alissa I, Nair AB, Aldhubiab B, Shah H, Shah J, Mewada V, *et al.* Design, Development, and Evaluation of Treprostinil Embedded Adhesive Transdermal Patch. Pharmaceutics. 2023;15(4):1226. doi:10.3390/pharmaceutics15041226
28. Srikakulam SR, Devineni J, Mokkapati C, Venigalla Y, Pothuri A, Acchi A, *et al.* A Novel Targeted Nanoliposomal Atorvastatin Transdermal Patch Assisted with Solid Microneedles for Improved Bioavailability. Ind J Pharm Edu Res. 2024;58(3):736-50. doi:10.5530/ijper.58.3.82
29. Zhang Y, Kung CP, Iliopoulos F, Sil BC, Hadgraft J, Lane ME. Dermal Delivery of Niacinamide-*in vivo* Studies. Pharmaceutics. 2021;13(5):726. doi:10.3390/pharmaceutics13050726
30. Dubrovin EV, Klinov DV, Schäffer TE. Evidence of (anti)metamorphic properties of modified graphitic surfaces obtained in real time at a single-molecule level. Colloids Surf B Biointerfaces. 2020;193:111077. doi:10.1016/j.colsurfb.2020.111077.
31. Debelec-Butuner B, Oner E, Kotmakci M, Kantarci AG. SIRT1 siRNA-loaded lipid nanoparticles enhanced doxorubicin-induced cell death in prostate cancer cell lines. J Drug Deliv Sci Technol. 2021;66:102670. doi:10.1016/j.jddst.2021.102670.
32. Lee MS, Han CS, Min KH, Kim DW, Park CW, Weon KY, *et al.* Development of Drug-in-Adhesive Patch Formulation for Transdermal Delivery of Pelubiprofen. Pharmaceutics. 2025;17(12):1580. doi:10.3390/pharmaceutics17121580
33. Dong W, Feng J, Liu X, Qu J, Li C, Li L, *et al.* Optimization and Evaluation of Colchicine Patch Formulation Based on Box-Behnken Design. AAPS PharmSciTech. 2025;26(6):188. doi:10.1208/s12249-025-03158-9
34. Taghizadeh SM, Moghimi-Ardakani A, Mohamadnia F. A statistical experimental design approach to evaluate the influence of various penetration enhancers on transdermal drug delivery of buprenorphine. Journal of Advanced Research. 2015;6(2):155-62. doi:10.1016/j.jare.2014.01.006
35. Škerget M. Supercritical Fluid Adsorption and Desorption of Lipids on Various Adsorbents. Acta Chim Slov. 2007;54(4):688-92.
36. Mo L, Lu G, Ou X, Ouyang D. Formulation and development of novel control release transdermal patches of carvedilol to improve bioavailability for the treatment of heart failure. Saudi Journal of Biological Sciences. 2022;29(1):266-72. doi:10.1016/j.sjbs.2021.08.088
37. Ilić T, Pantelić I, Lunter D, Đorđević S, Marković B, Ranković D, *et al.* Critical quality attributes, *in vitro* release and correlated *in vitro* skin permeation-*in vivo* tape stripping collective data for demonstrating therapeutic (non)equivalence of topical semisolids: A case study of "ready-to-use" vehicles. International Journal of Pharmaceutics. 2017;528(1-2):253-67. doi:10.1016/j.ijpharm.2017.06.018
38. Rui X, Okamoto Y, Fukushima S, Morishita Watanabe N, Umakoshi H. Investigating the impact of 2-OHOA-embedded liposomes on biophysical properties of cancer cell membranes via Laurdan two-photon microscopy imaging. Sci Rep. 2024;14(1):15831. doi:10.1038/s41598-024-65812-9

Cite this article: Shinde A, Gurav N, More H. Optimization of Palbociclib Nano Structured Lipid Carriers Loaded Transdermal Patch with Comprehensive *ex vivo* Skin Permeation and Retention Research for Management of Breast Cancer. Indian J of Pharmaceutical Education and Research. 2026;60(4s):s1486-s1497.